Drop-Size Distributions and Mie Computations for Rain

Christian Mätzler

Research Report No. 2002-16
November 2002

Institut für Angewandte Physik — Mikrowellenabteilung

Sidlerstrasse 5
3012 Bern
Schweiz

Tel. : +41 31 631 89 11
Fax. : +41 31 631 37 65
E-mail : matzler@iap.unibe.ch

rain2.doc

Drop-Size Distributions and Mie Computations for Rain

Christian Mätzler,
Institute of Applied Physics, University of Bern, Switzerland
November 2002

Contents

Abstract

The technical and scientific advancements in active and passive microwave remote sensing, covering the frequency range from roughly 1 to 1000 GHz, open the potential for quantitative studies, modelling and simulations. This applies also to precipitation. First of all, self-consistent drop-size distribution functions are required. For this purpose, the distributions of Laws-Parsons, Marshall-Palmer, Joss-Drizzle and Joss-Thunderstorm are analysed in view of an analytic expression for the terminal fall velocity in vertically stagnant air. It is found that all distributions need a rain-rate and pressure-dependent normalisation to fulfil the rain-rate integral equation. Secondly, Mie computations for extinction, absorption, scattering, back-scattering and asymmetric scattering are made with the 4 normalised distributions over the frequency range from 1 to 1000 GHz, using the dielectric model of liquid water by Liebe et. al. (1991). Characteristic differences between size distributions are found. Finally, due to the multiple dependencies of the microwave interaction with rain, it is concluded that tuned computations are more appropriate than look-up tables. Applications of this work include the design of new sensors and improved forward models for remote sensing of rain rate, rain-water content, and also to distinguish between different size distributions and thus for advancing physical cloud and precipitation models.

Introduction

During the last two decades, the development of active and passive microwave remote sensing achieved significant advancements. On the technical side they are based on improvements in stability and accuracy of phase and amplitude measurements with radar, radiometers and line-of-sight transmission links. On the modelling side, the radiative-transfer and propagation theory advanced as well, e.g. in the development of the atmospheric Microwave Propagation Model (MPM) over the frequency range from 1 to 1000 GHz by Liebe (1981) to Liebe et al. (1993), with further adjustments by Rosenkranz (1998) and by collaborative work in Europe, e.g. COST Action 712 in microwave radiometry (Mätzler, 2000), and efforts to develop software tools, such as ARTS (Bühler et al. 2002).

To take full advantage of these results in the observation of precipitation, it is necessary to advance precipitation studies to a similar level of accuracy. Such work will be beneficial for physical process studies of precipitation and for its parameterisation in numerical weather-prediction and climate models. Firstly, we need improved formulations of the drop-size distribution functions, including shape effects and fall velocity. In this paper emphasis is put on the size distribution of effective spherical drops, of their fall velocity and their interaction with microwave radiation in terms of Mie Theory.

As discussed by Pruppacher and Klett (1978), the evolution of rain-drop sizes is governed by complex processes, depending on parameters changing from the source region in clouds to the bottom of the atmosphere. Therefore, attempts to quantify the size distribution are mostly empirical. Still taken as a standard are the pioneering measurements by Laws and Parsons (1943) used to derive the distribution function of Marshall and Palmer (1948). The instrument of Laws and Parsons consisted of a layer of flour in which rain drops fell to form dough pellets, whose size was related to the droplet volume. The experiments and their analysis were very tedious. Similar size distributions followed later from an automated instrument, the disdrometer, developed by Joss and Waldvogel (1967), leading to the Drizzle (JD) and the Thunderstorm (JT) Distributions of Joss et al. (1968) for extreme forms of rain. Exponential functions were applied to all these observations. Because the functions are simple, their use has been attractive with a long tradition in rain-radar applications. However, it was pointed out on occasions that the exponential functions overestimate the size distribution at diameters below 1 to 2 mm, especially near the surface. This disadvantage was of minor concern to investigators with radars at decimetre and centimetre wavelengths where the signal was dominated by the largest drops. However, as the wavelength got shorter in radar and even more in radiometer applications, a reassessment of the size distributions was more and more required. This was the motivation of de Wolf (2001) who found that the modified gamma distribution allows better fits to the Laws-Parsons (LP) data than the exponential function. Another deficiency of the standard size distributions is that they are not properly normalised, i.e. the rain rate computed with these functions does not agree with the rain-rate variable. Such functions are not self consistent. The problem was pointed out by Olsen et al. (1978) and by de Wolf (2001) who proposed rain-rate dependent modifications of the original distribution functions. Here, the normalisation is reanalysed, using an improved function for the fall velocity, and taking into account its dependence on air pressure. Expressions are derived for 4 major distribution functions with normalisations accurate to 0.2% (assuming no error in fall velocity). See Annexe for a description of the MATLAB Functions.

The new functions are applied to the determination of microwave extinction, scattering and absorption by rain, using a recent software tool for Mie Computations in MATLAB (Math Works, 1992) developed by Mätzler (2002b, c). Until recently, tabular and graphical data, e.g. from Deirmendjian (1969), or simplified formulas with tabulated coefficients, e.g. by Olsen et al. (1978) for the extinction coefficient, have been in use. In view of the multiple dependencies on physical parameters, such as frequency, diameter, dielectric constant, temperature and pressure, it is advantageous to use direct Mie computations tuned to the respective situations. Such computations are sufficiently fast on modern computers. Furthermore, numerical simulations can easily include model modifications, e.g. impurity effects in the dielectric model of water.

Current rain drop-size distributions and their normalisation

Drop-size distribution

For a given rain rate R, the drop-size distribution function $N(D,R)$ describes the differential number of drops of diameter D per unit volume and per differential diameter range dD. The number N_V of drops per unit volume and the volume fraction f_V of rain water in air are given by the moments in D of $N(D,R)$ of order zero and three, respectively:

$$N_V = \int_0^\infty N(D,R)dD; \quad f_V = \frac{\pi}{6}\int_0^\infty D^3 N(D,R)dD \tag{1}$$

The measured size distribution of Laws and Parsons (1943) was represented as a fraction δF of the total rain-water volume in a given diameter range ($D,d+dD$):

$$\delta F = \frac{\pi}{6 f_V} D^3 N(D,R)\delta D \tag{2}$$

where δD was 0.25 mm. Assuming the fall velocity can be represented by a function of D, such as the terminal fall velocity V_∞ in stagnant air, the downward flux density of the rain-water volume is given by

$$R_N(R,P) = \frac{\pi}{6}\int_0^\infty D^3 N(D,R) V_\infty(D,P)dD \tag{3}$$

R_N has units of velocity. For a normalised distribution function, R_N is equal to the rain rate R, expressed as a velocity, mostly in mm/h. Thus, for R_N=R, Equation (3) is the rain-rate integral equation; if equality does not exist, the ratio

$$Norm(R,P) = \frac{R}{R_N(R,P)} \tag{4}$$

is used to transform $N(D,R)$ to the normalised distribution function $N_N(D,R,P)$:

$$N_N(D,R,P) = Norm(R,P)\cdot N(D,R) \tag{5}$$

which fulfils the rain-rate integral equation. Examples will be shown below.

Terminal fall velocity of raindrops

The quality of normalisation depends on the ability to describe the effective fall velocity of the raindrops. In the past, power-law expressions of the form, $V_\infty = aD^b$, were favoured, as they allowed to represent R_N by a moment in D of N. An example is the laminar Stokes velocity for which b=2 (Sauvageot, 1992). Unfortunately, the Stokes formula is limited to a very small range of diameters, typically <0.04mm, and a more realistic representation of V_∞ is given by the following formula for a standard air pressure of P_0=1013 hPa:

$$V_\infty(D,P_0) = \begin{cases} 0; & D \le 0.03mm \\ 4.323(D - 0.03mm); & 0.03mm < D \le 0.6mm \\ 9.65 - 10.3\exp(-0.6D); & D > 0.6mm \end{cases}; \quad (D \text{ in mm}) \tag{6}$$

The third expression, valid for D>0.6mm, is from Atlas et al. (1973) and has been widely used (Sauvageot, 1992). However, negative values are obtained for D<0.03mm. The second expression is used to avoid this problem; it is a linear fit to measurements of Gunn and Kinzer (1949), allowing for a smooth transition to the expression of Atlas. The first expression in (6) avoids negative values of the second one. With decreasing air pressure, the terminal fall velocity increases as shown in Figure 1. The variation can be modelled by (7)

$$V_\infty(D,P) = V_\infty(D,P_0)\cdot\left(\frac{P_0}{P}\right)^{0.291+0.0256D} \quad ; \quad (P_0 = 1013 \text{ hPa}, D \text{ in mm}) \tag{7}$$

where the exponent is slightly dependent on D. As an alternative, a constant exponent of about 0.35 can be used, especially when concentrating on the range of D values relevant in the size-distribution functions.

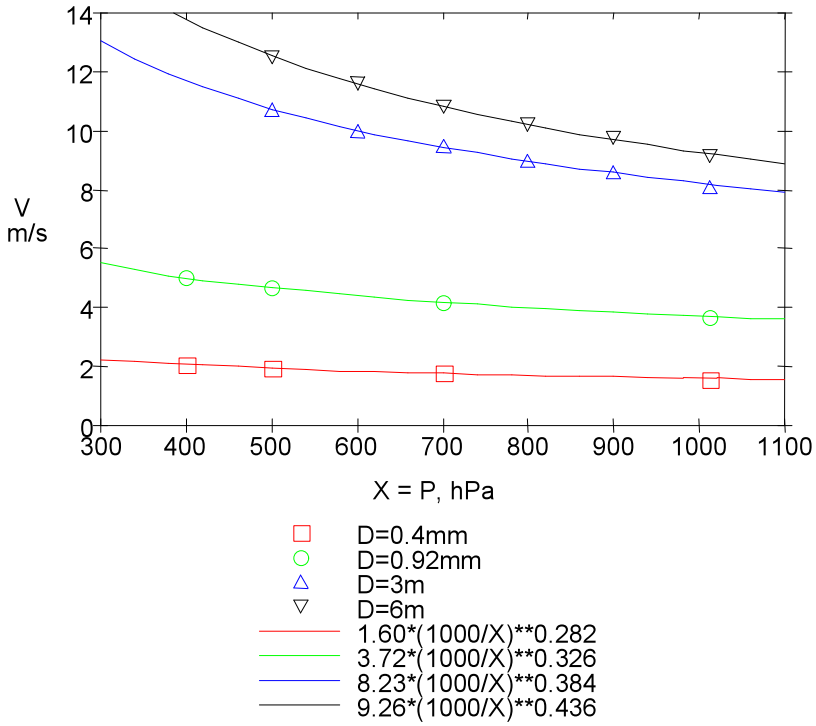

Figure 1: Terminal fall velocity versus air pressure, for D = 0.4, 0.92, 2 and 6 mm, according Figures 2.6 and 2.7 of Sauvageot, 1992, based on Beard and Pruppacher (1969), Beard (1976), and fitted functions to the data.

Empirical expressions for N(D,R) and N_N(N,R,P)

Empirical expressions considered here are of the form

$$N(D,R) = N_0 D^a \exp(-\Lambda D) \tag{8}$$

where N_0 and Λ are functions of R. For standard pressure P_0, the parameters of the normalised functions are shown in Table 1, where $Norm(R,P_0)$ is fitted by second-order polynomials in X=ln(R), and ln is the natural logarithm of R.

Table 1: Parameters of Equations (5) and (8) for normalised distributions at standard pressure P_0: LP according to de Wolf (2001), Marshall and Palmer (MP), Joss-Drizzle (JD) and Joss-Thunderstorm (JT) from Joss et al. (1968).

Distribution Function	$N_0(R)$; 1/mm^4	$Norm(R,P_0)$; X=ln(R), R in mm	$\Lambda(R)$; 1/mm	a
LP	$1.98\cdot10^{-5}R^{-0.384}\cdot Norm$	$1.047-0.0436\cdot X+0.00734\cdot X^2$	$5.38\cdot R^{-0.186}$	2.93
MP	$0.80\cdot10^{-5}\cdot Norm$	$0.842-0.00915\cdot X+0.0072\cdot X^2$	$4.1\cdot R^{-0.21}$	0
JD	$3.00\cdot10^{-5}\cdot Norm$	$1.1194-0.0367\cdot X+0.0079\cdot X^2$	$5.7\cdot R^{-0.21}$	0
JT	$0.14\cdot10^{-5}\cdot Norm$	$1.0945+0.0052\cdot X+0.0124\cdot X^2$	$3.0\cdot R^{-0.21}$	0

With increasing altitude, the air pressure decreases, and V_∞ increases according to Equation (7). Ignoring the weak D dependence in the exponent of the pressure ratio in (7), Equations (3) and (4) allow us to express the pressure dependence of *Norm* by

$$Norm(R,P) = Norm(R,P_0)\cdot\left(\frac{P}{P_0}\right)^{0.35}; \qquad (P \text{ in hPa},\ P_0 = 1013 \text{ hPa}) \qquad (9)$$

where the exponent 0.35 is an effective mean value, corresponding to the dominant drop diameters between 1 and 3 mm. Together with functions $Norm(R,P_0)$ of Table 1, Equation (9) is used to transform the original size distributions (8) to the normalised ones of Equation (5) for any D, P and R.

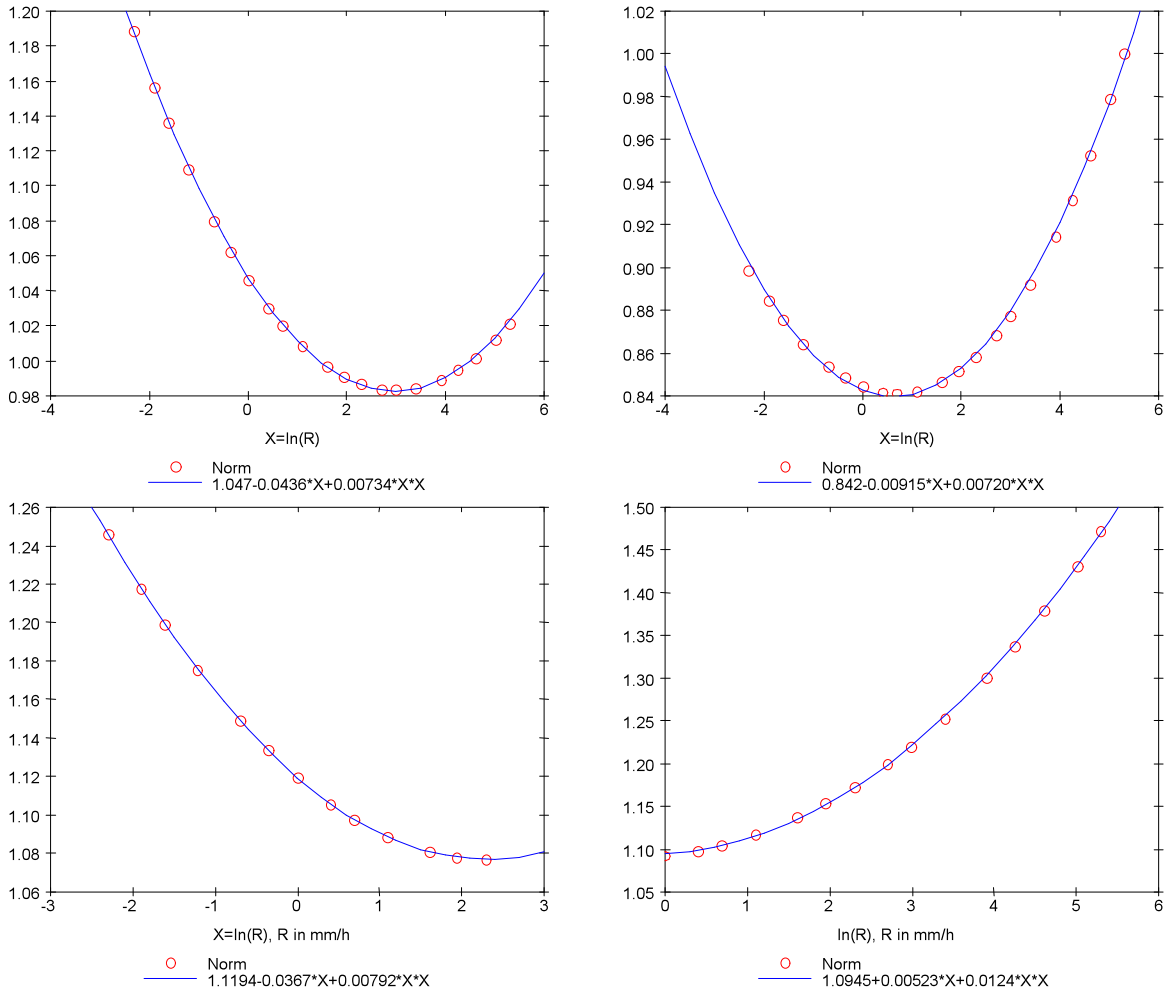

Figure 2: Computed and fitted $Norm(R,P_0)$ values versus X=ln$R$ of size distributions of LP (top left), MP (top right), JD (bottom left) and JT (bottom right) for adapted ranges of R.

The fits to the actual *Norm* values are displayed in Figure 2. The standard deviation of the fits is 0.002 or smaller. The normalisation, being a correction on the order of 20% for LP, MP and JD, and up to 50% for JT, is a significant improvement of the original functions to errors of about 0.2%, assuming V_∞ to be correct. The four rain-distribution functions are shown in the semi-logarithmic plot of Figure 3 for R=5mm/h together with the distribution function of a cloud (Cumulus Congestus) with a liquid-water content of 0.8g/m^3 (Ulaby et al. 1981). MP is the exponential (straight line) fit to LP whose slope is between the two Joss distributions, indicating the range of slopes from drizzle to thunderstorm. When comparing with the cloud function, it appears that the total distribution of rain and cloud must be closer to an exponential than to LP. Therefore the exponential function may be a better choice for the effective

size distribution in source regions. On the other hand, clouds are usually absent near the bottom of the atmosphere, where most rain-size distributions are measured. There the LP distribution is realistic. Broad access to this distribution was given in form of δF values by Skolnik (1990) in his Table 23.2 from Burrows and Attwood (1949). These data are used to test the present LP function, by computing δF values with (2). The comparisons for different rain rates are shown in Figure 4, again for standard pressure. There is a good correspondence, especially at the higher rain rates.

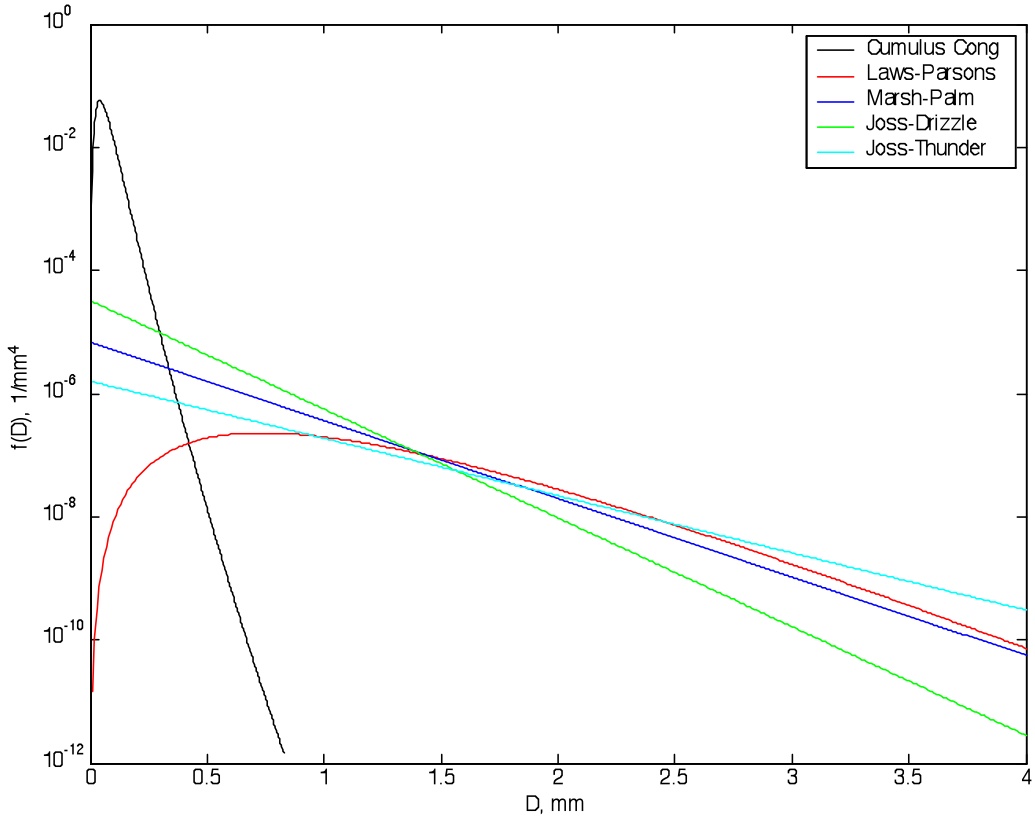

Figure 3: Normalised LP (red), MP (blue), JD (green) and JT (cyan) distributions versus D for R=5mm/h, P=P_0. Also shown is a typical size distribution of a cloud (black): Cumulus Congestus.

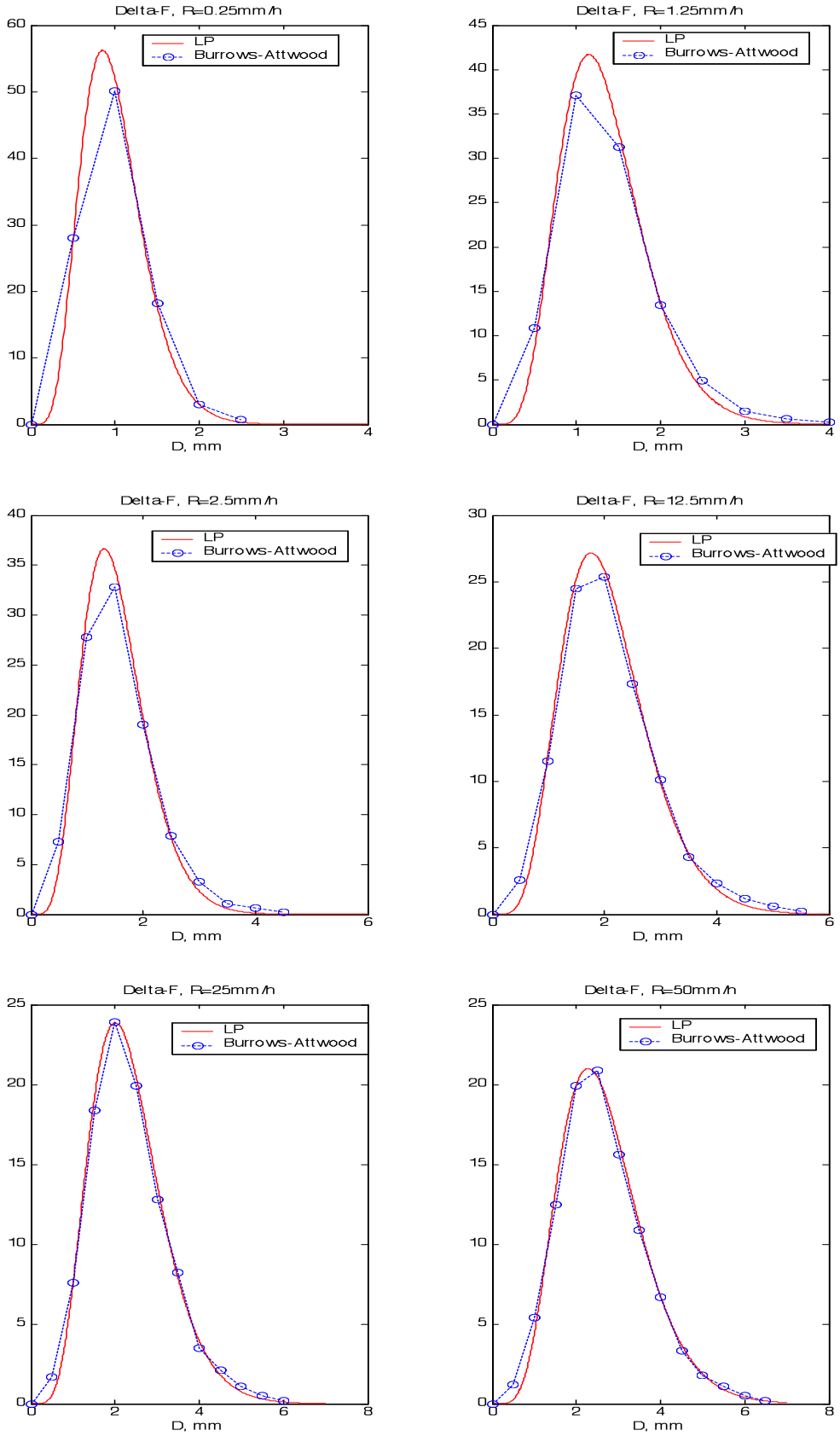

Figure 4: Volume-fraction δF in % of total rain volume for droplet diameter range centred at *D*, with δ*D*=0.5mm, for rain rates of 0.25 to 50mm/h: blue circles are data or Burrows and Attwood (1949), red curves and dots represent the normalised LP Distribution.

Size-distribution effects in Mie computations

How much do extinction and backscattering of microwave radiation depend on the actual choice of the distribution function? This question was studied by Olsen et al. (1978) and by Crane and Burke (1978), s. also Nathanson et al. (1991). Here, the question is generalised to all basic scattering parameters (coefficients for extinction, scattering, backscattering, absorption or emission, and asymmetric scattering), assuming that the rain drops are spherical, pure-water droplets. Then the theory of Mie (1908) is adequate. Apart from the size information, Mie Theory needs the complex refractive index of non-magnetic spheres, such as water drops. The complex refractive index $m(\nu,T)$, being a function of frequency ν and temperature T, is related to the complex relative dielectric permittivity $\varepsilon(\nu,T)$ by

$$m(\nu,T) = \sqrt{\varepsilon(\nu,T)} \tag{10}$$

In contrast to earlier investigations which were mostly based on the refractive data of water by Ray (1972), a newer and more accurate model is used here, namely the dielectric function of Liebe et al. (1991), covering the frequency range from 1 to 1000 GHz.

For Mie computations of rain, a set of MATLAB (Math Works, 1992) Functions was developed by Mätzler (2002b, c), based on the Formulation of Bohren and Huffman (1983). Modified versions of these functions will be used here.

The quantities we are looking for are the interaction cross sections by rain per unit volume of a rainy atmosphere, i.e. the coefficients for rain extinction γ_{ext}, scattering γ_{sca}, absorption γ_{abs}, backscattering γ_b, and asymmetric scattering $\gamma_{asy}=<\cos\vartheta>\gamma_{sca}$, all expressed in units of 1/km. Here, $<\cos\vartheta>$ is the effective cosine of the scattering angle. To convert the coefficients to dB/km they have to be multiplied with a factor of 4.343. The coefficients γ_j, *j=ext, sca, abs, b, asy*, can be computed from the corresponding Mie Efficiencies Q_j and the size distribution

$$\gamma_j = 0.25\pi \int_0^\infty D^2 Q_j(D) N(D) dD \tag{11}$$

The integrands of (11)

$$\frac{d\gamma_j}{dD} = 0.25\pi D^2 Q_j(D) N(D) \tag{12}$$

show how much the droplets of a given diameter contribute to γ_j. As a first example, the situation of the 4 distributions at ν=94 GHz, T=277K, R=2.5mm/h is shown in Figure 5, and a second example of 2 distributions of the same rain situation is shown in Figure 6 at the much lower frequency of ν=9.4 GHz. All quantities are peaked at D=values between 0.7 and 2.3 mm. A closer look shows significant variations between distribution functions: At 94 GHz, the maximum of the function for extinction changes from less than 0.35/km/mm to 1/km/mm, whereas at 9.4 GHz the extinction is similar for both LP and MP, and also for JD and JT (not shown). Whereas at 94 GHz absorption is about half of the extinction, at 9.4 GHz both are nearly equal. In contrast to MP, JD, JT of Figure 5, there are practically no contributions at $D \leq 0.5$mm for LP. This is a consequence of the suppression of small drops in LP. In contrast to other cases, in JD there are practically no contributions at $D \geq 2.5$mm. At 94 GHz, the functions for the scattering and absorption coefficients are very similar in LP; on the other hand, for MP and even more for JD, the absorption clearly dominates over scattering due to the larger number of small drops.

When Figures 4, 5 and 6 are compared, it is found that there is a certain similarity, especially between δF and extinction or absorption. However the back- and asymmetric scattering parameters show a distinctly different behaviour. This is one of the reasons why radar data are poorly correlated with water volume and rain rate.

Size effects are also visible in the integral values, the coefficients of Equation (11). This is shown versus rain rate in the graphs of Figures 7 and 8, again for the cases of T=277K, 94 and 9.4 GHz, respectively. The behaviour of JT is similar to LP, both curves being flatter at 94 GHz than JD and MP. An opposite behaviour is observed at 9.4GHz.

Spectra of extinction, scattering, absorption and backscattering coefficients are shown in the graphs of Figure 9 for R=2.5mm/h. The dominance of all quantities of the Joss-Drizzle (JD) Distribution at frequencies above 80 GHz is apparent, whereas an opposite behaviour is observed at low frequencies for the scattering and backscattering coefficient. Extinction and absorption are characterised by S-shaped spectra, leading to significant enhancements with respect to Rayleigh Theory already at frequencies of about 10 GHz.

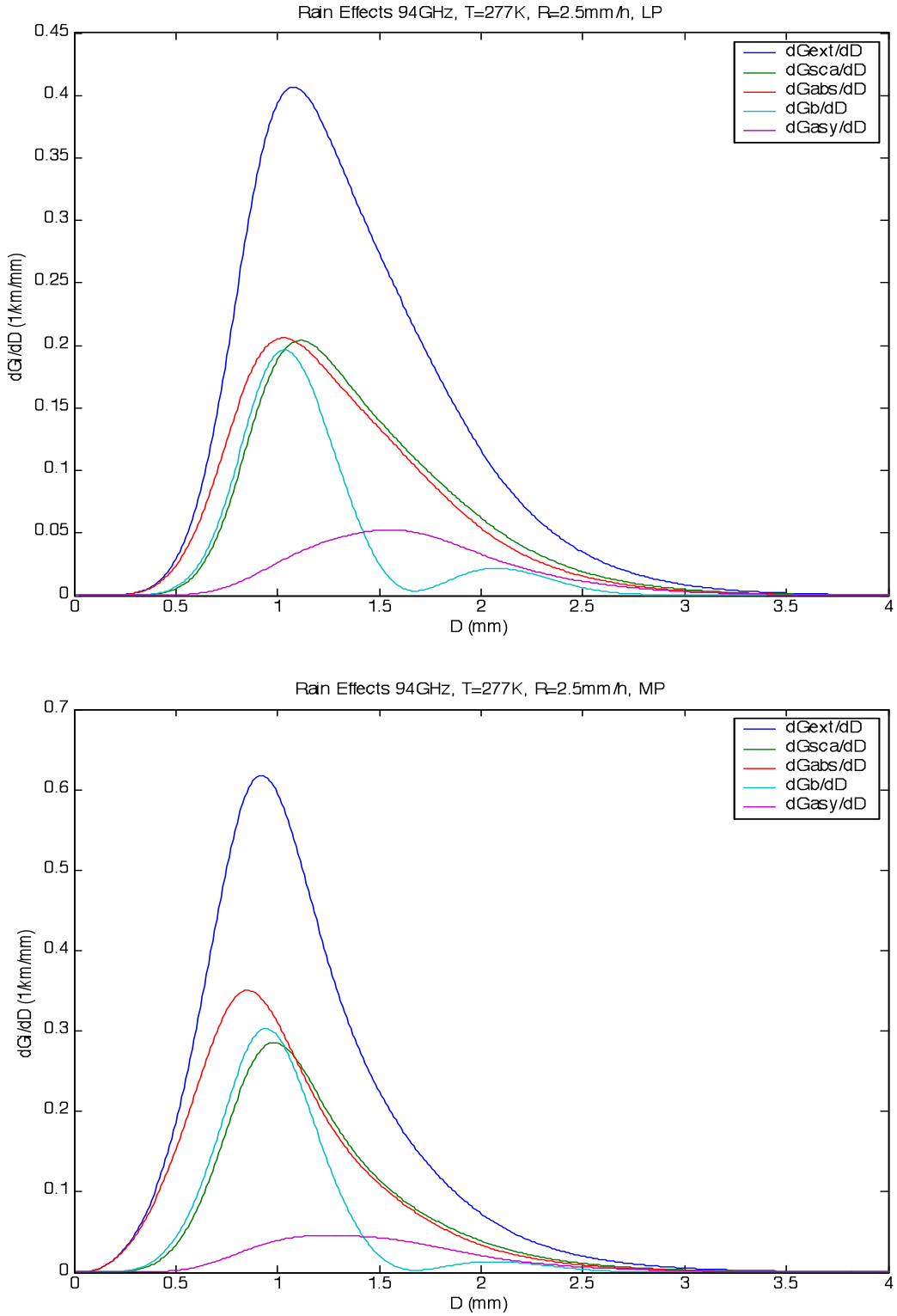

Figure 5: Integrands of extinction γ_{ext}, scattering γ_{sca}, absorption γ_{abs}, and backscattering coefficients γ_b, and of asymmetric scattering $\gamma_{asy}=\gamma_{sca}\langle\cos\theta\rangle$, versus drop diameter D at T=277K, $P=P_0$, R=2.5mm/h, ν=94 GHz for LP (top) and MP (bottom) drop-size distribution.

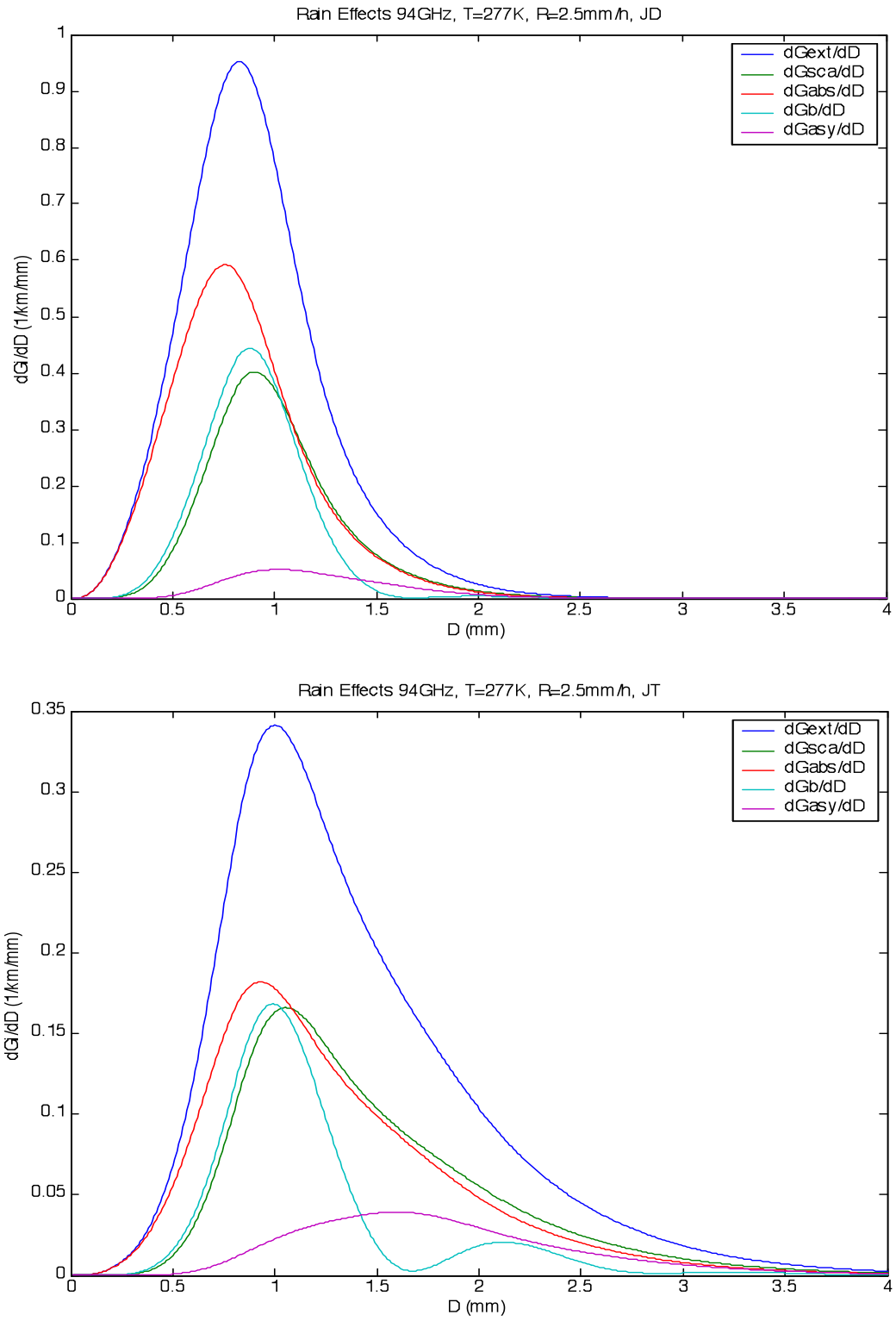

Figure 5 continued: Integrands of extinction γ_{ext}, scattering γ_{sca}, absorption γ_{abs}, and backscattering coefficients γ_b, and of $\gamma_{asy}=\gamma_{sca}\langle\cos\theta\rangle$, versus drop diameter D at T=277K, $P=P_0$, R=5mm/h, ν=94 GHz for Joss Distributions JD (top) and JT (bottom).

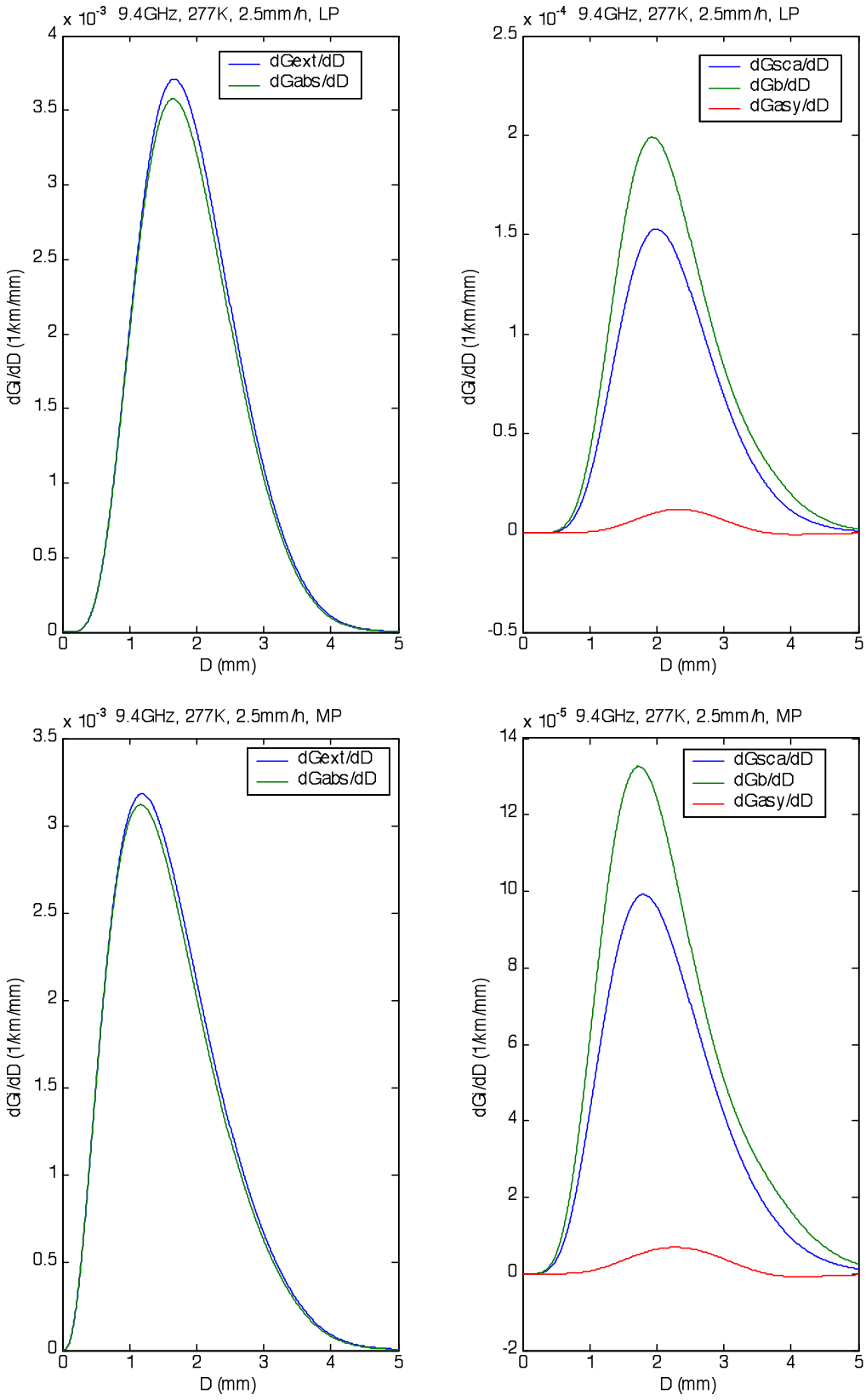

Figure 6: Integrands of extinction γ_{ext}, absorption γ_{abs}, backscattering coefficients γ_b, scattering γ_{sca}, and of asymmetric scattering γ_{asy}, versus drop diameter D at T=277K, P=P_0, R=2.5mm/h, ν=9.4 GHz for LP (top) and MP (bottom) drop-size distribution.

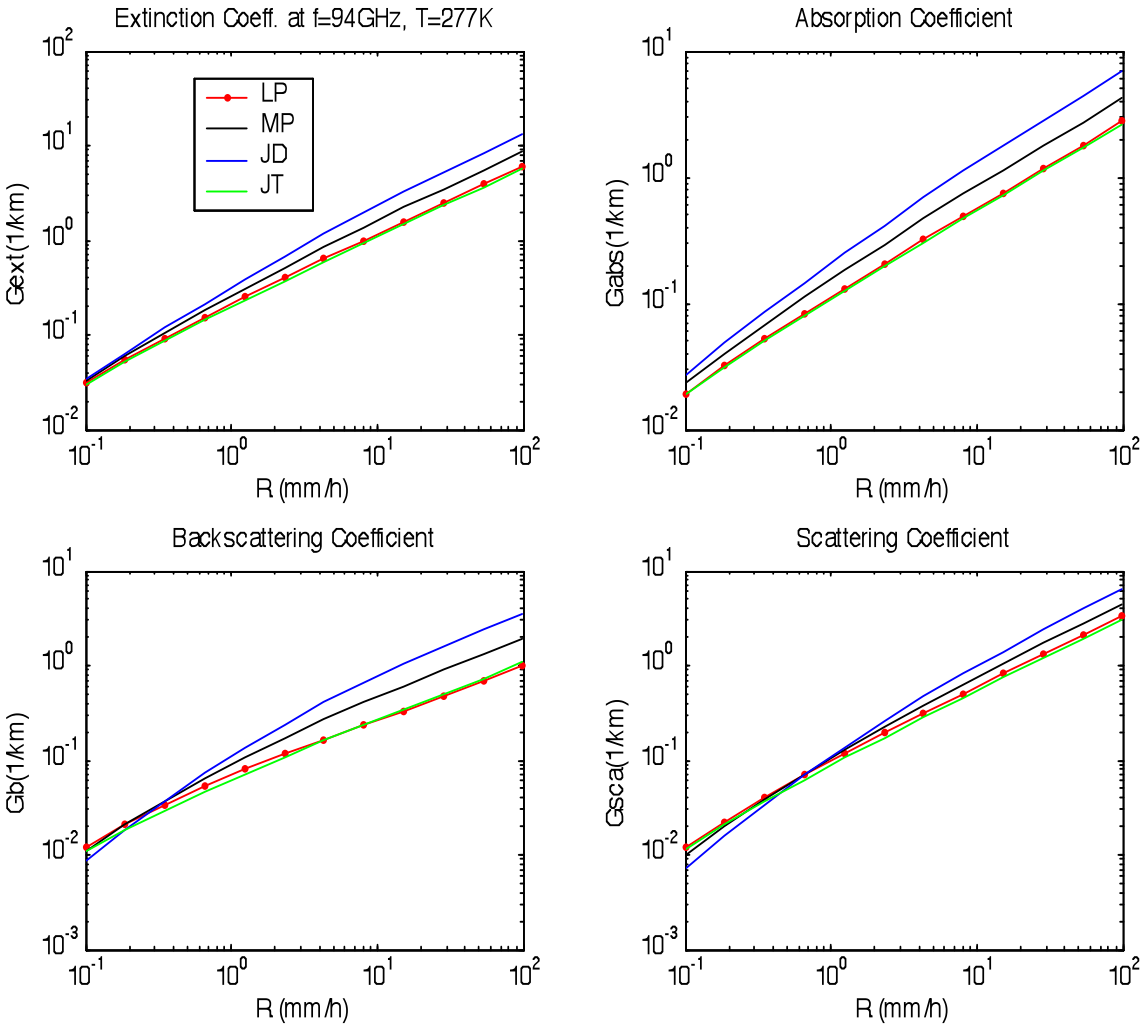

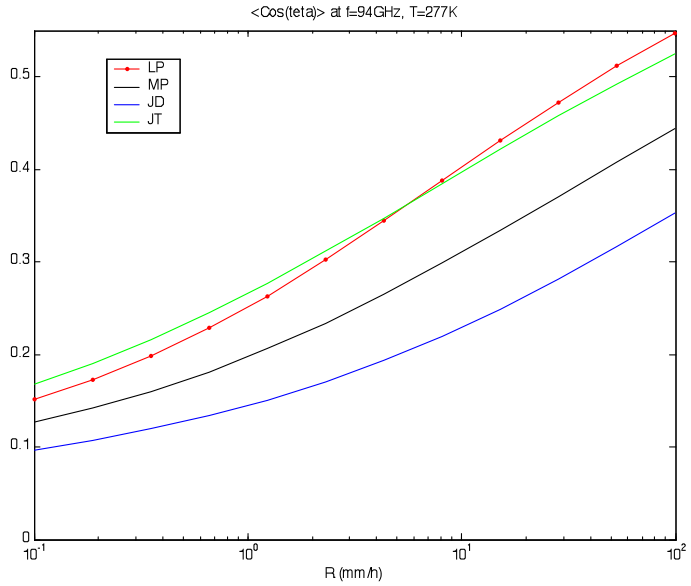

Figure 7: Extinction γ_{ext}, absorption γ_{abs}, backscattering γ_b and scattering coefficient γ_{sca}, all in 1/km, versus rain rate at 94 GHz, T=277K, P=P_0 for the four distribution functions. Also shown is the effective cosine of the scattering angle for the same situations.

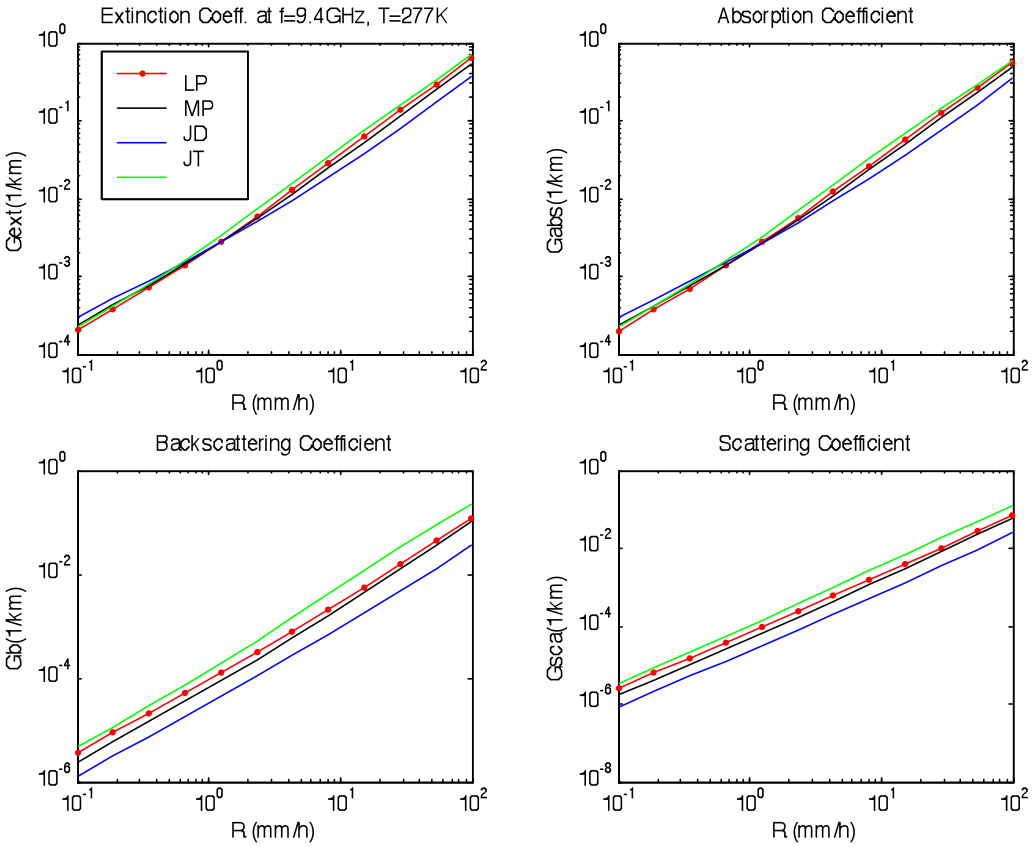

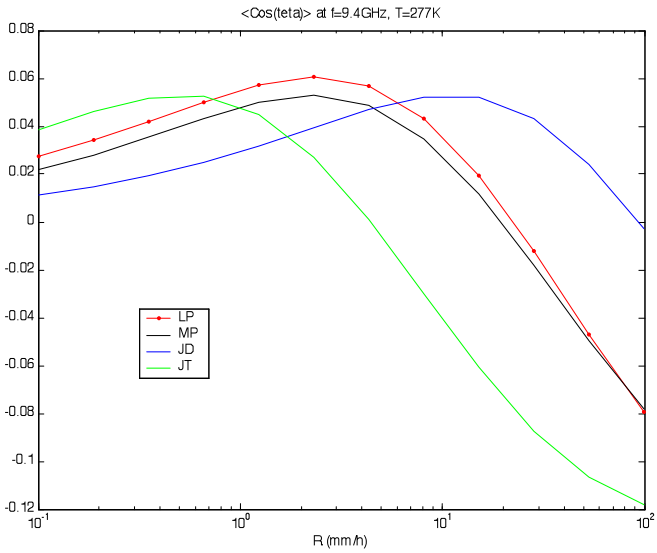

Figure 8: Extinction γ_{ext}, absorption γ_{abs}, backscattering γ_b and scattering coefficient γ_{sca}, all in 1/km, versus rain rate at 9.4 GHz, T=277K, P=P_0 for the four distribution functions. Also shown is the effective cosine of the scattering angle for the same situations.

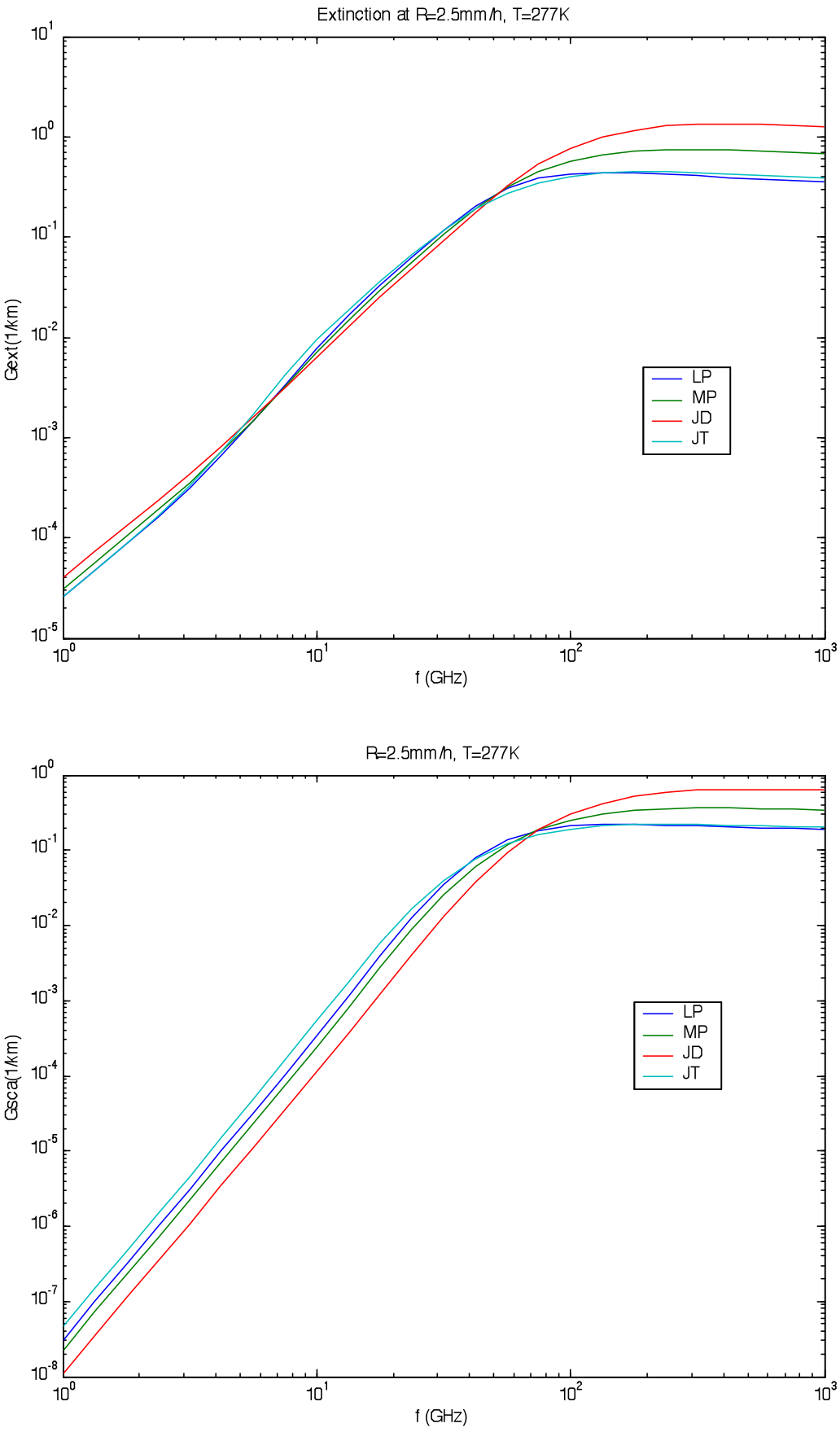

Figure 9 : Spectra of extinction (top) and scattering (bottom) coefficients at T=277K, P=P_0, R=2.5mm/h for the four distribution functions LP, MP, JD and JT.

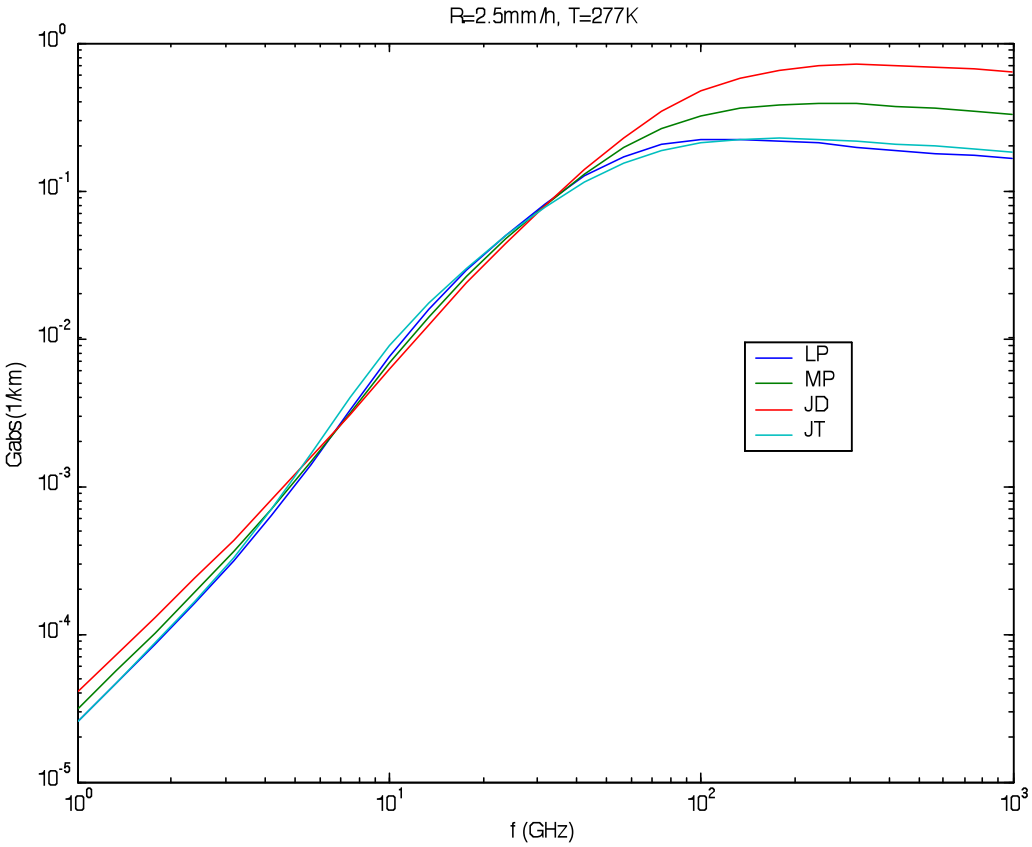

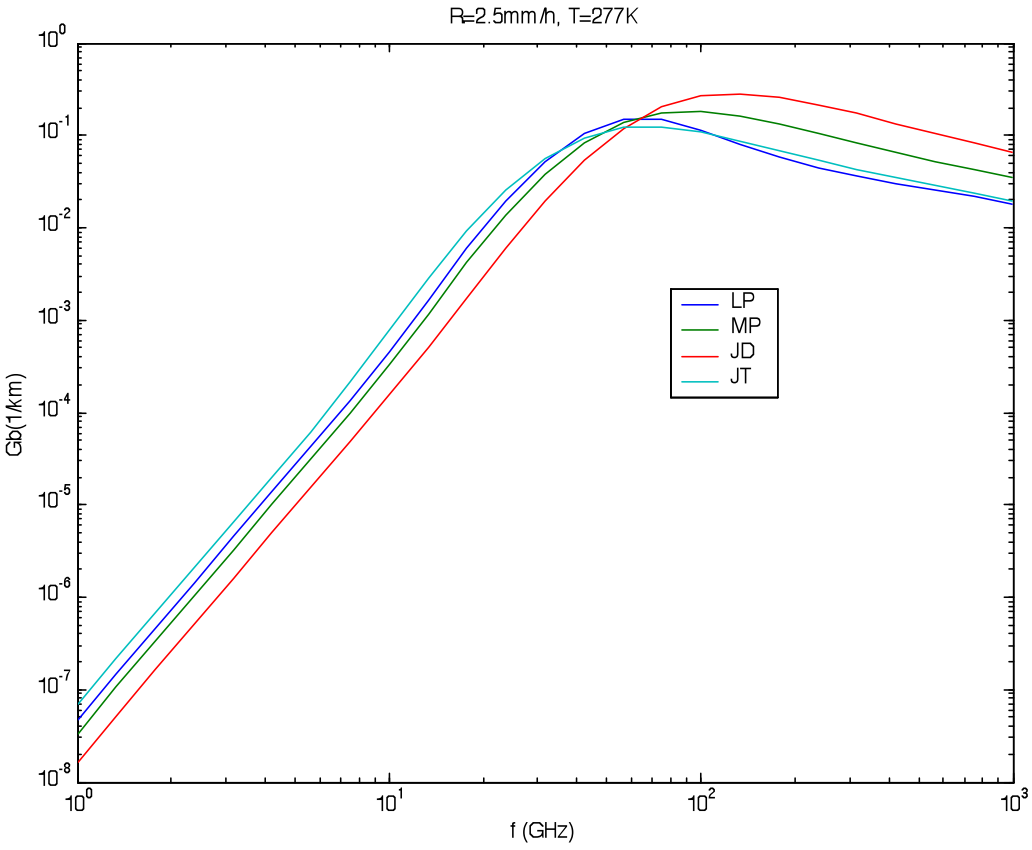

Figure 9, continued: Spectra of absorption (top) and backscattering (bottom) coefficients at T=277K, $P=P_0$, R=2.5mm/h for the four distribution functions LP, MP, JD and JT.

Conclusions

Four different size distribution functions of rain drops were analysed for rain rates from 0.1 to 100 mm/h in view of an analytic expression for the terminal fall velocity in vertically stagnant air. It was found that all distributions need a rain-rate and pressure-dependent normalisation to fulfil the rain-rate integral equation to within 0.2%. The results are given by Equations (5), (8), (9) and Table 1. The use of consistent distribution functions helps to improve the accuracy of remote sensing by radar, radiometry and line-of-sight transmission measurements.

Mie computations made over the frequency range from 1 to 1000 GHz show characteristic differences between the four size distributions. Only some effects were addressed here. The potential of the MATLAB Tools prepared for the present work (see Annexe for a short description) is much wider. It is a basis for forward models for advanced measurements of rain rate, rain water content, vertically integrated rain-water content, to distinguish between different size distributions and for sensitivity studies in the design of new sensors.

A limitation imposed by the present work is the consideration of spherical water drops. Effects of non-sphericity were ignored or reduced to an equivalent sphere size. The increasing oblateness of rain drops with increasing drop size, and thus with increasing rain rate, leads to polarisation effects in both, scattering and absorption, and thus in extinction (e.g. Sauvageot, 1992; Olsen et al. 1978). Such effects can easily be handled in the Rayleigh Approximation (Mätzler, 2002a) with limitations to frequencies up to about 10 GHz. On the other hand, at very high frequencies, the anisotropy effect is almost negligible. In the intermediate range the computation of scattering by non-spherical particles is a difficult task. However, results for precipitation indicate that minor standard corrections (dependent on polarisation, frequency and rain rate) of Mie Theory allow sufficiently accurate computations (e.g. Olsen et al. 1978).

The accuracy also depends on the fall velocity. Here we used a new expression, valid for vertically stagnant air. As long as rain is not correlated with the positions of updrafts and downdrafts, the assumption is reasonable. Questionable is the present normalisation of the distribution functions in regions where precipitation is generated, because these are often rising cloud layers or convectively rising sections of clouds where complex processes, including the ice phase, govern rain formation. Therefore the present work cannot directly be applied to the source region. Nevertheless, the significant sensitivities of radiative properties on the distribution functions found here encourage the application of microwave radar, radiometers and line-of-sight transmission links for precipitation studies, including precipitation sources. Such work is needed for the quantitative understanding of the physical processes occurring in the atmosphere.

References

Atlas D., R.C. Srivastava, and R.S. Sekhon, “Doppler radar characteristics of precipitation at vertical incidence”, Rev. Geophys. 11, 1-35 (1973).

Beard K.V., “Terminal fall velocity and shape of cloud and precipitation drops aloft”, J. Atmos. Sci. Vol. 33, pp. 851-864 (1976).

Beard K.V. and H.R. Pruppacher, “A determination of terminal velocity and drag of small water drops by means of a wind tunnel ”, J. Atmos. Sci. Vol. 26, pp. 1066-1072 (1969).

Bohren C.F. and D.R. Huffman, “Absorption and Scattering of Light by Small Particles”, John Wiley, New York, NY (1983).

Burrows C.R. and S.S. Attwood, “Radio wave propagation”, Consolidated technical report of the Committee on Propagation, NDRC, Academic Press, New York, p. 219 (1949).

Bühler S., P. Eriksson, W. Haas, N. Koulev, T. Kuhn and O. Lemke, “ARTS User Guide”, Version 1.0.38, Download from http://www.sat.uni-bremen.de/arts/, University of Bremen, Aug. 2002.

Crane R.K. and H.K. Burke, “The evaluation of models for atmospheric attenuation and backscatter characteristic estimation at 95 GHz”, Environ. Res. and Technol. Doc. No. P-3606, Feb. (1978).

Czekala H., S.Crewell, C.Simmer and A.Thiele, “Discrimination of cloud and rain liquid water path by ground-based microwave radiometry”, Geophys. Res. Letters 28(2), 267-270, 2001.

Deirmendjian, D. “Electromagnetic Scattering on Spherical Polydispersions”, American Elsevier, New York, NY (1969).

de Wolf D.A. “On the Laws-Parsons distribution of raindrop sizes”, Radio Science Vol.36, No. 4, pp. 639-642 (2001).

Gunn R. and G.D. Kinzer, “The terminal velocity of fall for water droplets in stagnant air”, J. Meteorology, 6, 243-248 (1949).

Joss J. und A. Waldvogel, “Ein Spektrograph für Niederschlagstropfen mit automatischer Auswertung”, Pure Applied Geophys., 68, pp. 240-246 (1967).

Joss, J., J.C. Thams, and A. Waldvogel, “The variation of rain-drop size distributions at Locarno”, in Proc. Internat. Conf. on Cloud Physics, 369-373 (1968).

Laws J.O. and D.A. Parsons, “The relationship of raindrop size to intensity”, Trans. AGU, 24, 452-460 (1943).

Liebe H.J., “Modeling attenuation and phase of radio waves in air at freequencies below 1000 GHz”, Radio Sci. Vol. 16, pp. 1183-1199 (1981).

Liebe H.J., G.A. Hufford and T. Manabe, “A model for the complex permittivity of water at frequencies below 1 THz”, Internat. J. Infrared and mm Waves, Vol. 12, pp. 659-675 (1991).

Liebe, H.J., G.A. Hufford, and M.G. Cotton, Propagation Modeling of Moist Air and Suspended Water/Ice Particles at Frequencies Below 1000 GHz. AGARD Conference Proc. 542, Atmospheric Propagation Effects through Natural and Man-Made Obscurants for Visible to MM-Wave Radiation, pp.3.1-3.10 (1993).

Marshall J.S. and W. Palmer, “The distribution of rain drops with size”, J. Meteorology, 5, 165-166 (1948).

Math Works, “MATLAB User’s Guide”, Natick, MA (1992).

Mätzler C. (ed.) "Radiative transfer models for microwave radiometry", COST Action 712 "Application of microwave radiometry to atmospheric research and monitoring", Meteorology, Final Report of Project 1, European Commission, Directorate General for Research, EUR 19543, ISBN 92-828-9842-3 (2000).

Mätzler, C. “Radarsignale von anisotropem Niederschlag ”, IAP Res. Rep. No. 02-2, April (2002a).

Mätzler C. “Effects of rain on propagation, absorption and scattering of microwave radiation based on the dielectric model of Liebe”, IAP Res. Rep. No. 02-10, June (2002b).

Mätzler C. “MATLAB Functions for Mie Scattering and Absorption, Version 2”, IAP Res. Rep. No. 02-11, August (2002c).

Mie G. “Beiträge zur Optik trüber Medien, speziell kolloidaler Metallösungen“, Annals of Physics, Vol. 25, pp. 377-445 (1908).

Nathanson F.E., J.P. Reilly, and M.N. Cohen, “Radar Design Principles“, 2nd Ed., McGraw-Hill (1991).

Olsen R.L., D.V. Rogers and D.B. Hodge, “The aR^b relation in the calculation of rain attenuation”, IEEE Trans. Ant. Prop. Vol. AP-26, pp. 318-329 (1978).

Pruppacher H.R. and J.D. Klett, “Microphysics of clouds and precipitation”, Reidel, Dordrecht, Holland (1978).

Rosenkranz, P. W., Water vapor microwave continuum absorption: A comparison of measurements and models, Radio Science, **33**, pp. 919-928 (1998). Correction, Radio Science, **34**, p. 1025 (1999).

Sauvageot H., “Radar Meteorology”, Artech House, Boston, MA (1992).

Ulaby F.T., R.K. Moore and A.K. Fung, "Microwave Remote Sensing, Active and Passive", Vol. 1, Artech House, Dedham, MA-U.S.A. (1981).

Annexe: Computer Functions and Programs for Rain

Remark: For general Mie Computations, see Mätzler (2002c).

MATLAB Function for the terminal fall velocity in stagnant air: rainfallspeed

```
function result = rainfallspeed(D)

% Terminal fall speed in m/s of rain drops of diameter D in mm
% adapted from Sauvageot (1992)
% C. Mätzler, Oct. 2002.
```

MATLAB Functions for raindrop size distributions: rainXY

```
function result = rainLP(R,D)

% Laws and Parsons (LP) drop-size distribution, fitted by
% de Wolf, Radio Sci. 36, 639 (2001), Equation (7)
% but with additional normalisation, s. Factor y.
% Input:
% R: Rain rate or line vector of rain rates, in mm/h
% D: diameter or column vector of diameters, in mm
% C. Mätzler, Oct. 2002.

function result = rainMP(R, D)

% Marshall-Palmer (MP) drop-size distribution
% with normalisation by Matzler
% Input:
% R: Rain rate or line vector of rain rates, in mm/h
% D: diameter or column vector of diameters, in mm
% C. Mätzler, Oct. 2002.

function result = rainJD(R, D)

% Joss-Drizzle (JD) drop-size distribution
% with normalisation by Matzler
% Input:
% R: Rain rate or line vector of rain rates, in mm/h
% D: diameter or column vector of diameters, in mm
% C. Mätzler, Oct. 2002.

function result = rainJT(R, D)

% Joss-Thunderstorm (JT) drop-size distribution
% with normalisation by Matzler
% Input:
% R: Rain rate or line vector of rain rates, in mm/h
% D: diameter or column vector of diameters, in mm
% C. Mätzler, Oct. 2002.
```

Main function for Mie computations of rain: Mie_rain

```
function result = Mie_rain(fGHz, R, TK, distribution)

% Mie- extinction, scattering, absorption, backscattering
% and asymmetric scattering coefficients in 1/km
% for normalised drop-size distributions.
% Input:
% fGHz: frequency in GHz,  range 1 to 1000 GHz
% R: Rain rate in mm/h,    range 0.1 to 100 mm/h
% TK: Temp. in K,          range 260 to 310 K
% distribution:
% 'LP' for Laws-Parsons, 'MP' for Marshall-Palmer,
% 'JD' for Joss-Drizzle, or 'JT' for Joss-Thunderstorm
% C. Mätzler, Oct. 2002
```

Figure 3: plotdistributions

```
function result = plotdistributions(R,dmax,Dmax)

% Plot of rain and cloud distribution functions
% R: Rain rate in mm/h,
% dmax: max. cloud-droplet diameter in mm
% Dmax: max. rain-droplet diameter in mm
% C. Mätzler, Nov. 2002.
```

Plotting pairs of graphs of Figure 4: raintestLPx2

```
function result = raintestLPx2(nt,dD)

% Test of Laws and Parsons (LP) drop-size distribution
% of de Wolf, Radio Sci. 36, 639 (2001), Equation (7)
% with additional renormalisation, s. Factor y.
% Test results to be plotted and returned.
% Input:
% nt: number of data pair (1, 2 or 3) to be selected
% dD incremental diameter for plot of distr. function, in mm
% C. Mätzler, Oct. 2002.
% Data from Burros and Attwood, 149, Table 23.2 in
% M.I.Skolnik, Radar Handbook, 2nd Edition, 1990:
```

Figure 5: Mie_rain2

```
function result = Mie_rain2(fGHz, R, TK, dD, Dmax, distribution)

% Weighting functions of
% Rain extinction, scattering, absorption, backscattering and
% asymmetric scattering coefficient in 1/km/mm versus drop diameter
% for different drop-size distributions (Sauvageot et al. 1992),
% using Mie Theory, and dielectric model of Liebe et al. 1991.
% Input:
```

```
% fGHz: frequency in GHz,
% R: rain rate in mm/h, TK: Temp. in K, incremental diameter dD in mm,
% Dmax: maximum diameter in mm
% distribution='LP' for Laws-Parsons, 'MP' for Marshall-Palmer,
% 'JD' for Joss-Drizzle, or 'JT' for Joss-Thunderstorm
% C. Mätzler, June 2002.
```

Figure 6: Mie_rain2a

```
function result = Mie_rain2a(fGHz, R, TK, dD, Dmax, distribution)

% Dual plot of weighting functions of
% Rain extinction, scattering, absorption, backscattering and
% asymmetric scattering coefficient in 1/km/mm versus drop diameter
% for different drop-size distributions (Sauvageot et al. 1992),
% using Mie Theory, and dielectric model of Liebe et al. 1991.
% Input:
% fGHz: frequency in GHz,
% R: rain rate in mm/h, TK: Temp. in K, incremental diameter dD in mm,
% Dmax: maximum diameter in mm
% distribution='LP' for Laws-Parsons, 'MP' for Marshall-Palmer,
% 'JD' for Joss-Drizzle, or 'JT' for Joss-Thunderstorm
% C. Mätzler, Nov. 2002.
```

Figures 7 and 8: Mie_rain3d (Graphs 1 to 4)

```
function result = Mie_rain3d(fGHz, TK, nrain, dD, nsteps)

% 4 X plot of
% Extinction, scattering, absorption, backscattering
% coefficients in 1/km versus rain rate,
% using Mie Theory, and Liebe '91 dielectric model for water.
% for 4 different size distribution functions:
% Laws-Parsons, Marshall-Palmer, Joss-Drizzle, Joss-Thunderstorm
% Input:
% fGHz: frequency in GHz, TK: temperature in K,
% nrain: Number of rain rates between Rmin=0.1 and Rmax=100mm/h
% dD, nsteps: diameter step size and number of steps
% C. Mätzler, June 2002, revised Nov. 2002.
```

Figures 7 and 8: Mie_rain3e (Graph 5)

```
function result = Mie_rain3d(fGHz, TK, nrain, dD, nsteps)

% Cosine of effective scattering angle versus rain rate, R,
% using Mie Theory, and Liebe '91 dielectric model for water.
% for 4 different size distribution functions:
% Laws-Parsons, Marshall-Palmer, Joss-Drizzle, Joss-Thunderstorm
% Input:
% fGHz: frequency in GHz, TK: temperature in K,
```

```
% nrain: Number of rain rates between Rmin=0.1 and Rmax=100mm/h
% dD, nsteps: diameter step size and number of steps
% C. Mätzler, June 2002, revised Nov. 2002.
```

Rain spectra: Mie_rain4

```
function result = Mie_rain4(R, TK, fmin, fmax, nfreq, dist)

% Extinction, scattering, absorption, backscattering and
% asymmetric scattering coefficients in 1/km for a selected
% drop-size distribution 'dist' (Sauvageot et al. 1992),
% versus frequency, using Mie Theory and dielectric Model of
% Liebe et al. 1991, Input:
% R: rain rate in mm/h, TK: Temp. in K,
% fmin, fmax: minimum and maximum frequency in GHz
% nfreq: Number of log-spaced frequencies between fmin and fmax
% dist='LP' for Laws-Parsons, 'MP' for Marshall-Palmer,
% 'JD' for Joss-Drizzle, or 'JT' for Joss-Thunderstorm
% C. Mätzler, June 2002, rev. Oct. 2002.
```

Figure 9: Mie_rain4a

```
function result = Mie_rain4a(R, TK, fmin, fmax, nfreq, sel)

% Spectra of either extinction, scattering, absorption,
% backscattering or asymmetric scattering coefficients
% in 1/km for the 4 drop-size distributions LP, MP, JD, JT
% using Mie Theory and dielectric Model of Liebe et al. 1991
% Input:
% R: rain rate in mm/h, TK: Temp. in K,
% fmin, fmax: minimum and maximum frequency in GHz
% nfreq: Number of log-spaced frequencies between fmin and fmax
% sel='ext', 'sca', 'abs', 'b', or 'asy' to select a Mie Propagation Parameter
% C. Mätzler, June 2002, rev. Oct. 2002.
```